

Unregulated ARF6 Activation in Epithelial Cysts Generates Hyperactive Signaling Endosomes and Disrupts Morphogenesis

Jogender S. Tushir,^{*†‡} James Clancy,^{*†} Andrew Warren,^{*} Carolyn Wrobel,^{§||} Joan S. Brugge,[§] and Crislyn D'Souza-Schorey^{*}

^{*}Department of Biological Sciences, University of Notre Dame, Notre Dame, IN 46556; and [§]Department of Cell Biology, Harvard Medical School, Boston MA 02115

Submitted September 29, 2009; Revised April 29, 2010; Accepted May 3, 2010
Monitoring Editor: Jean Schwarzbauer

Tumor development in glandular tissues is associated with structural alterations in the hollow ducts and spherical structures that comprise such tissues. We describe a signaling axis involving sustained activation of the GTP-binding protein, ARF6, that provokes dramatic changes in the organization of epithelial cysts, reminiscent of tumorigenic glandular phenotypes. In reconstituted basement membrane cultures of renal epithelial cysts, enhanced ARF6 activation induces the formation of cell-filled glandular structures with multiple lumens and disassembled cadherin-based cell–cell contacts. All of these alterations are accompanied by growth factor receptor internalization into signaling endosomes and reversed by blocking ARF6 activation or receptor endocytosis. Receptor localization in signaling endosomes results in hyperactive extracellular signal-regulated kinase signaling leading to Bcl-2 stabilization and aberrant cysts. Similarly, formation of hyperproliferative and disorganized mammary acini induced by chronic stimulation of colony-stimulating factor 1 receptor is coupled to endogenous ARF6 activation and constitutive receptor internalization and is reversed by ARF6 inhibition. These findings identify a previously unrecognized link between ARF6-regulated receptor internalization and events that drive dramatic alterations in cyst morphogenesis providing new mechanistic insight into the molecular processes that can promote epithelial glandular disruption.

INTRODUCTION

Glandular epithelial organs are comprised of monolayers of adherent cells that enclose hollow lumens. These lumen enclosing glandular structures organize to form spherical cysts or cylindrical tubules, which are topologically equivalent at many levels. Each cell in a fully developed cyst (also known as acini in the mammary gland, follicles in the thyroid, and alveoli in the lung) or tubule, has a free apical surface oriented toward the lumen, a lateral surface that adheres to the adjacent cell and a basal surface that is in contact with the underlying extracellular matrix directly, or through an outer epithelial cell layer (Bissell *et al.*, 2003). It has been proposed that the establishment of these three membrane surfaces by each cell in a self enclosed monolayer is intrinsic to epithelial tissue differentiation and the establishment of glandular architecture (O'Brien *et al.*, 2002). Lumen formation has been thought to occur predominantly by two processes: cavitation, where the lumen is generated by apoptosis of cells in the

middle of the glandular structure, and hollowing, a process wherein space is created by exocytosis and separation of apposing apical membranes (O'Brien *et al.*, 2002; Mailleux *et al.*, 2008). Thus, to generate epithelial glands, a wide range of cellular processes, including proliferation, polarization, cell–cell and cell–matrix adhesion, secretion, and cell death, must be precisely coordinated both spatially and temporally.

Many epithelial cancers are associated with disruption of normal epithelial glandular architecture. Histological phenotypes associated with altered epithelial glands include filled lumens, loss of polarization, disruption of cell–cell contacts, and acquisition of invasive behavior (Bissell *et al.*, 2003; Debnath and Brugge, 2005). Although many of these structural perturbations are observed in both early stage and invasive epithelial cancers, little is known about the molecular mechanisms and cellular events that lead to these pathological phenotypes. Many of the cellular processes that culminate in epithelial glandular development are controlled by signaling responses induced by growth factors that serve as activating ligands for membrane receptors. Elevated receptor activity resulting from increased expression or activating mutations leads to constitutive signaling that could disrupt glandular organization during disease progression (Debnath and Brugge, 2005).

ARF6 is a member of the ARF family of Ras-related GTPases and has been shown to control endocytic traffic and actin remodeling in a variety of cell types (D'Souza-Schorey and Chavrier, 2006). In epithelial cells, ARF6 has been shown to function downstream of hepatocyte growth factor (HGF) and Src activation to promote E-cadherin endocytosis

This article was published online ahead of print in *MBoC in Press* (<http://www.molbiolcell.org/cgi/doi/10.1091/mbc.E09-09-0824>) on May 26, 2010.

[†] These authors contributed equally to this work.

Present addresses: [‡] University of Massachusetts Medical School, Worcester, MA; ^{||} Department of Biological Sciences, DePaul University, Jackson, IL.

Address correspondence to: Crislyn D'Souza-Schorey (d'souza-schorey.1@nd.edu).

during adherens junction disassembly and cell migration (D'Souza-Schorey, 2005). Furthermore, loss of epithelial phenotype and acquisition of a migratory phenotype is accompanied by elevated pools of ARF6-GTP in cells (Palacios and D'Souza-Schorey, 2003). More recent work has shown that the ARF6 exchange factor GEP100, which facilitates GTP loading on ARF6, is expressed in 70% of primary breast ductal carcinomas, and it is preferentially coexpressed with epidermal growth factor receptor (EGFR) in malignant tumors (Morishige *et al.*, 2008). Here, we report on the induction of signaling responses and cellular alterations induced as a consequence of unregulated ARF6 activation in reconstituted basement membrane cultures of renal and mammary epithelial cysts, and we describe mechanisms by which blocking ARF6 function restores normal glandular phenotype. The ability of epithelial cells to adopt tissue-like conformations when grown in a three-dimensional (3D) extracellular matrix has made 3D cell culture a powerful approach to investigate the mechanisms that cause the disruption of these structures. The findings reported here are particularly significant given that ARF6 as well as phospholipase D (PLD) activation has been shown to correlate with epithelial tumor progression (D'Souza-Schorey and Chavrier, 2006; Rodrik *et al.*, 2006; Zheng *et al.*, 2006).

MATERIALS AND METHODS

Cell Culture and Maintenance

Madin Darby canine kidney (MDCK) cells were maintained in DMEM supplemented with 10% fetal bovine serum, penicillin, and streptomycin. Growth conditions for MDCK cells expressing hemagglutinin (HA)-tagged ARF6-Q67L and ARF6-T27N, MDCK^{ARF6-Q}, and MDCK^{ARF6-T} respectively, under control of the tetracycline-repressible transactivator have been described previously (Prigent *et al.*, 2003). Cells were maintained in the presence of 1 μ g/ml doxycycline (Dox) or switched to Dox-free medium to induce expression of ARF6 proteins. ARF6 mutant proteins are expressed within 24 h after induction (Tushir and D'Souza-Schorey, 2007). MCF10A cells expressing colony-stimulating factor 1 receptor (CSF-1R) receptors have been described previously (Shaw *et al.*, 2004; Wrobel *et al.*, 2004).

Cyst Development Assays

Growth of MDCK cysts in 3D cultures was performed as described previously (Tushir and D'Souza-Schorey, 2007). MCF-10A cysts were cultured as described previously (Wrobel *et al.*, 2004). For both cell cultures, single cell suspensions of 4×10^3 cells are overlaid on Matrigel seeded in a well of an eight-well chamber slide. Developing MDCK cysts were continuously fed every 36 h with fresh medium until mature cysts were formed. For MCF-10A cysts expressing CSF-1R, assay media containing 10 ng/ml CSF-1 were replaced every 4 d unless indicated otherwise. To inhibit extracellular signal-regulated kinase (ERK) and PLD activities, 25 μ g/ml PD98059 or 0.5% 1-butanol, respectively, was added to the assay medium at day 4 after seeding. For morphological evaluations, for each experimental condition described, at least 200 cysts were examined and representative images are shown.

Plasmids, Antibodies, and Other Reagents

The expression plasmid ARF6(T27N)-HA-pCDNA3 has been described previously (Schweitzer and D'Souza-Schorey, 2002). The retroviral expression plasmid PLZRS-IRES-ARF6(T27N)/green fluorescent protein (GFP) also was described previously (Palacios *et al.*, 2001). Eps15(Eh29)-pEGFP was a gift from Alexander Benmerah (Institut Cochin, Paris, France). Primary antibodies used in these studies were anti-Bcl-2 mouse monoclonal (Millipore, Billerica, MA), anti-Bax rabbit polyclonal (Millipore), anti-phosphoserine rabbit polyclonal (Cell Signaling Technology, Danvers, MA), anti-Bim rabbit monoclonal (Cell Signaling Technology), anti-ERK1/2 mouse monoclonal (Cell Signaling Technology), anti-phospho-ERK1/2 rabbit polyclonal (Cell Signaling Technology), mouse anti-HA monoclonal (Covance Research Products, Princeton, NJ), anti-c-Met goat polyclonal used for immunofluorescent staining, and rabbit polyclonal used for Western blotting from Santa Cruz Biotechnology (Santa Cruz, CA); anti-Tfn-R mouse monoclonal (Zymed Laboratories, South San Francisco, CA); anti-CSF-1R rabbit polyclonal (Santa Cruz Biotechnology); anti-gp135 mouse monoclonal was from George Ojakian; anti-phospho-Akt polyclonal (Cell Signaling Technology), anti-phosphoserine (Millipore Bioscience Research Reagents, Temecula, CA); and anti-E-cadherin mouse monoclonal (Palacios *et al.*, 2001). HGF and PD98059 were obtained from

Calbiochem (San Diego, CA). CSF was from R&D Systems (Minneapolis, MN). High Pure RNA isolation kit (FastStart High Fidelity PCR systems) was from Roche Applied Sciences (Indianapolis, IN). iScript cDNA synthesis kit was from Bio-Rad Laboratories (Hercules, CA). The Caspase-Glo 3/7 kit was from Promega (Madison, WI). Matrigel was obtained from BD Biosciences (San Jose, CA). All other reagents were from Sigma-Aldrich (St. Louis, MO).

Immunofluorescence

The 3D cell cultures were processed for fixation, staining, and immunofluorescence as described previously (Tushir and D'Souza-Schorey, 2007). In brief, cysts were fixed in 4% paraformaldehyde followed by staining with primary antibody and then with fluorophore-conjugated secondary antibodies. Secondary antibodies used were goat anti-mouse fluorescein isothiocyanate (FITC), goat anti-mouse Texas Red, donkey anti-goat Cy3, goat anti-rabbit FITC, and goat anti-rabbit Texas Red (Invitrogen, Carlsbad, CA). Nuclei were stained using Draq5 (Alexis Biochemicals, San Diego, CA) or To-Pro3 (Invitrogen). Actin filaments were stained with either rhodamine-phalloidin or FITC-phalloidin (Invitrogen). Coverslips were mounted on glass slides using antifade mounting media (Invitrogen). Micrographs were obtained using a Diaphot 200 fluorescence microscope (Nikon, Tokyo, Japan) and an MRC 1024 scanning confocal and imaging system (Bio-Rad Laboratories).

Biochemical Analysis of Cysts

For generation of protein lysates for biochemical assays, cyst cultures were first treated with 0.25% trypsin to separate the glandular structures from Matrigel. Cells were then lysed in radioimmunoprecipitation assay (RIPA) buffer (150 mM sodium chloride, 1% IGEPAL CA-630, 0.5% sodium deoxycholate, 0.1% SDS, 50 mM Tris-HCl, and 1% mammalian protease inhibitor cocktail), and protein concentration was measured using the Bradford assay (Pierce Chemical, Rockford, IL). Equal amounts of protein were used for SDS-polyacrylamide gel electrophoresis (PAGE) followed by transfer to nitrocellulose membranes and Western blotting for detection of specific proteins. For immunoprecipitations, cysts were lysed in RIPA buffer as described above, and lysates were incubated with anti-Bcl-2 or anti-phosphoserine and then processed for immunoprecipitations as described previously (Tushir and D'Souza-Schorey, 2007). Immunoprecipitates were resolved by SDS-PAGE and probed with anti-ubiquitin or anti-Bcl-2 antibody as noted.

Assay for PLD Activity

Cellular lipids were labeled by incubating mature cysts in Opti-MEM, 0.5% fetal bovine serum, and 1.5 μ Ci/ml [³H]oleic acid for 18–24 h. Then, 0.5% butanol was added to the medium, and incubation continued for an additional 3 h. Cellular lipids were isolated by extraction with chloroform/methanol and separated by thin layer chromatography (TLC) on silica gel plates with H₂O-saturated ethyl acetate/isooctane/acetic acid (55:25:10) as solvent. The chromatogram was sprayed with α -naphthol/sulfuric acid to visualize phospholipids. Phosphatidylbutanol was identified by comigration with an unlabeled standard and quantitated by liquid scintillation counting.

Quantitative Reverse Transcription-Polymerase Chain Reaction (RT-PCR)

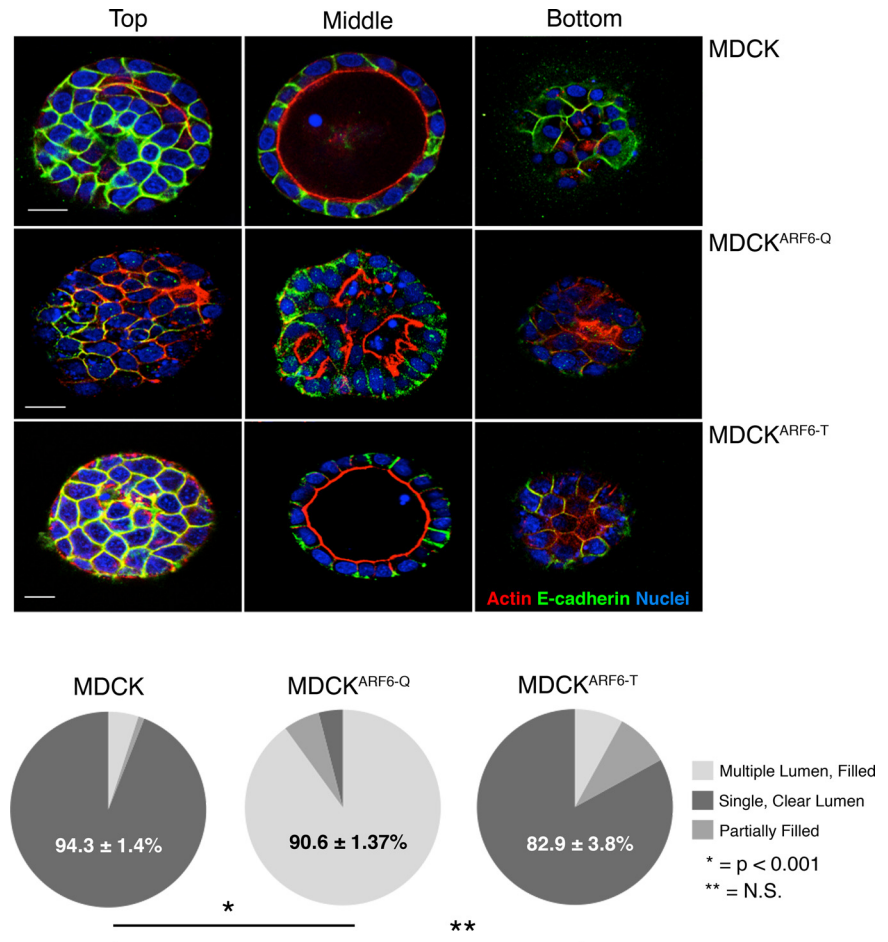
RNA was extracted from 3D cell culture lysates using High Pure RNA isolation kit (Roche Applied Sciences), and cDNA was generated using the iScript cDNA synthesis kit (Bio-Rad Laboratories). RT-PCR was performed as described previously (Tushir and D'Souza-Schorey, 2007). The following forward primer sequences were used: Bcl-2 forward (GGT GGA GGA GCT CTT CAG G) and Bcl-2 reverse (ACA GTT CCA CAA AGG CAT CC) and actin forward (ACT GGG ACG ACA TGG AGA AG) and actin reverse (CGT CGG GTA GTT CGT AGC TC). PCR products were quantitated using a NanoDrop-ND 1000 spectrophotometer (Thermo Fisher Scientific, Waltham, MA) and resolved on agarose gels.

RESULTS

Sustained ARF6 Activation Disrupts Cyst Lumen Clearance

To examine the effects of gain or loss of function of ARF6 during cyst development in 3D cultures, we used MDCK cell lines MDCK^{ARF6-Q} and MDCK^{ARF6-T} that express HA-tagged variants of the activated GTP-bound ARF6(Q67L) mutant, or the dominant-negative GDP-bound ARF6(T27N) mutant, respectively, under the control of a tetracycline-repressible transactivator. ARF6 mutant protein expression is observed 24 h after induction (Tushir and D'Souza-Schorey, 2007). When incubated in reconstituted basement membrane (Matrigel) for ~10 d, epithelial cells develop polarized cysts

Figure 1. Constitutive ARF6 activation perturbs cyst development. Parental MDCK, MDCK^{ARF6-Q}, and MDCK^{ARF6-T} cysts formed in 3D Matrigel culture were fixed and labeled for actin (red), E-cadherin (green), and nuclei (blue). MDCK and MDCK^{ARF6-T} cysts exhibit clear lumens whereas aberrant cysts with multiple lumens and internal cells are observed in MDCK^{ARF6-Q} cysts. Merged images of single confocal sections through the top, middle on bottom of each cyst type is shown. Bar, 10 μ m. Phenotypes as indicated were quantified by examining cysts in randomly selected fields by focusing through the z-axis. Cysts with single clear lumens were defined as those with only one lumen and free of internal cells. Multi lumen cysts were identified by the presence of multiple apical actin bands surrounding several smaller lumens. All cysts containing multiple lumens also contained internal cells. Partially filled cysts were distinguished by the presence of a strong apical actin band surrounding a single lumen that contained one or more internal cells. For each condition a minimum of 200 cysts were examined across several independent experiments. Values given are the mean and SE for the predominant phenotype in each condition. * $p < 0.001$ and **, not statistically significant.



with hollow lumens (Debnath *et al.*, 2003; Lee *et al.*, 2007). Here, MDCK cysts in Matrigel were monitored by analyzing single confocal sections taken through whole mounts of cysts. In fully developed cysts of parental MDCK cells, intense actin staining was appropriately localized to the free apical surface facing the lumen, and the cell–cell adhesion molecule E-cadherin localized to the basolateral membrane (Figure 1). The majority of MDCK^{ARF6-T} cells also formed normal cysts similar to parental cells (Figure 1). However, cells induced to express the ARF6-GTP mutant formed aberrant cysts. In the majority of MDCK^{ARF6-Q} cysts, some loss of cadherin-based adhesive contacts was observed along with cytoplasmic and punctate E-cadherin labeling (Figure 1, and additional images in Supplemental Figure 1). This is consistent with previous work showing that ARF6 activation promotes E-cadherin endocytosis to facilitate the disassembly of adherens junctions (D'Souza-Schorey, 2005). MDCK^{ARF6-Q} cysts had multiple lumens that were separated by cells that readily incorporated calcein AM, the membrane permeant fluorescent probe for viable cells (Supplemental Figure 2). Thus, sustained elevation of ARF6-GTP levels leads to marked alterations in cyst structures that resemble certain histological phenotypes seen in glandular epithelial tumors. These phenotypes were observed independent of cell density in 3D culture. In this regard, a fivefold increase or decrease in the number of cells seeded for culturing (see *Materials and Methods*) did not alter the phenotypes described above (our unpublished observations). Given the emerging evidence for a direct correlation between elevated

cellular ARF6-GTP pools and tumor progression we investigated the molecular basis of these abnormalities.

Sustained ARF6 Activation Prevents Loss of Prosurvival Signals during the Later Stages of Cyst Development

Because filling of cysts was a predominant phenotype induced by ARF6-GTP expression, we sought to investigate lumen development in MDCK^{ARF6-Q} cysts. For these studies, single cells were seeded in 3D culture and doxycycline was removed 48 h later to allow mutant ARF6 protein expression within 24 h. At this stage, normal cysts display apical–basal polarity. Biochemical and morphological analyses at subsequent stages of cyst development allowed us to more closely examine lumen development.

The importance of apoptosis or programmed cell death in creating and maintaining luminal spaces was first documented in the vertebrate embryo (Cocouvanis and Martin, 1995) and has since been noted in several *in vitro* systems, including MDCK cysts (Lin *et al.*, 1999). Prosurvival members of the Bcl-2 family delay or inhibit lumen formation when over expressed either alone or in combination with positive regulators of cell proliferation such as cyclin-D or HPV E7 (Debnath *et al.*, 2002). We examined the expression profile of prosurvival and proapoptotic proteins during development of MDCK^{ARF6-T} and MDCK^{ARF6-Q} cysts. As shown in Figure 2A, Western blotting of parental cyst lysates showed a steady decrease in Bcl-2 expression with significant down-regulation by day 5. In contrast, the expression of the proapoptotic protein, Bax (BH3 proteins

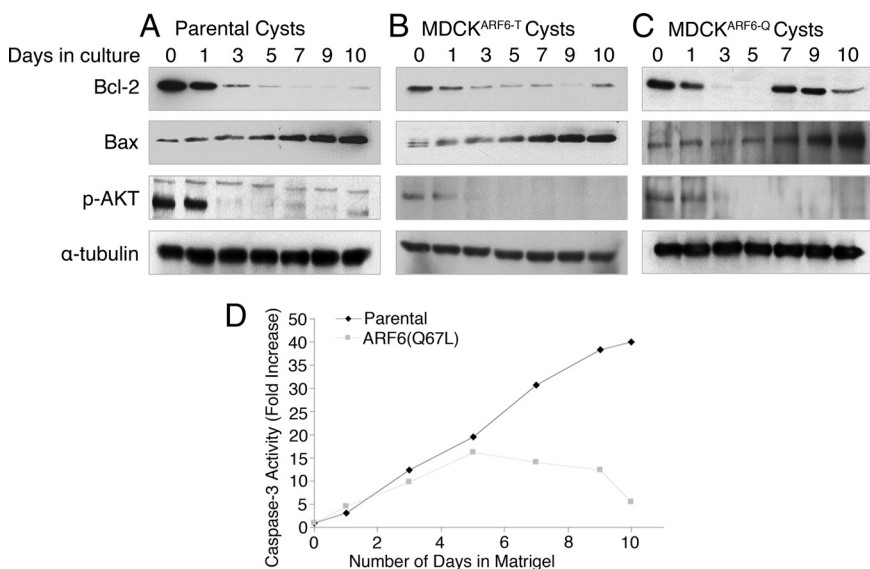


Figure 2. Reemergence of Bcl-2 expression in MDCK^{ARF6-Q} cysts. Parental MDCK (A), MDCK^{ARF6-T} (B), and MDCK^{ARF6-Q} (C) cells were seeded in Matrigel to develop into cysts. Two days after seeding, doxycycline was removed from the culture medium to allow mutant ARF6 expression. At the indicated number of days after seeding, developing cysts in culture were harvested, lysed, and quantitated for total protein. Equal amounts of cyst lysates were resolved on SDS-PAGE and then examined for expression of Bcl-2, Bax, and phospho-AKT by using Western blotting procedures. Lysates were also probed for α -tubulin to ensure equal loading. The data are representative of at least three independent experiments. Increased Bcl-2 expression was observed at late stages of cyst development in MDCK^{ARF6-Q} cysts.

1–3) was concomitantly up-regulated. The expression profile of the aforementioned proteins was almost identical in MDCK^{ARF6-T} cysts (Figure 2B). In contrast, MDCK^{ARF6-Q} cysts exhibited a reemergence of Bcl-2 expression during the later stages of cyst development (Figure 2C). This increased Bcl-2 expression could explain the presence of surviving cells in MDCK^{ARF6-Q} cyst lumens. In addition, caspase activity was markedly reduced during later stages of MDCK^{ARF6-Q} cyst development relative to normal cyst development (Figure 2D). The expression of Bax was unaffected in MDCK^{ARF6-Q} cysts.

ARF6-Induced ERK Activation Stabilizes Bcl-2 during the Later Stages of Cyst Development

To investigate the mechanism behind the reemergence of Bcl-2 expression in MDCK^{ARF6-Q} cysts, we first analyzed the effect of the ARF6-GTP mutant on Bcl-2 mRNA levels by quantitative RT-PCR. No changes in Bcl-2 transcription were observed in MDCK^{ARF6-Q} cysts (Supplemental Figure 3), suggesting that posttranscriptional regulation or an effect on protein stability may be responsible for Bcl-2 up-regulation.

We examined Akt (protein kinase B) activation because it has been shown to promote Bcl-2 expression and cell survival downstream of receptor tyrosine kinases (Breitschopf *et al.*, 2000; Pugazhenthii *et al.*, 2000; van Golen *et al.*, 2000). However, MDCK and MDCK^{ARF6-Q} cells exhibited overlapping profiles of phosphorylated Akt during cyst development (Figure 2, A–C), suggesting that signaling pathways downstream and/or independent of Akt facilitate the reemergence of Bcl-2 in MDCK^{ARF6-Q} cysts. Next, we examined stabilizing post-translational modifications of Bcl-2 in MDCK^{ARF6-Q} cysts. Phosphorylation of Bcl-2 at its loop domain has been shown to stabilize the protein even in the presence of cytotoxic signals, whereas mutation of the three consensus MAPK phosphorylation sites in the loop domain leads to ubiquitination of Bcl-2 and its subsequent degradation by the proteasome (Dimmeler *et al.*, 1999; Breitschopf *et al.*, 2000). Furthermore, ERK has been shown to have a role downstream of ARF6 during tumor cell invasion as well as epithelial tubule initiation (Tushir and D'Souza-Schorey, 2007; Muralidharan-Chari *et al.*, 2009). Thus, we tested the hypothesis that ARF6 activation increased ERK signaling during cyst development. As seen in Figure 3A, whereas

basal levels of ERK activation remained constant throughout cyst development in parental MDCK cysts, phosphorylated ERK levels were markedly increased in MDCK^{ARF6-Q} cysts. There is a slight enhancement at day 5 and then a robust increase by day 7, which is further sustained. We also examined components upstream in the Raf-mitogen-activated protein kinase kinase (MEK)-ERK signaling module and found that phosphorylated c-Raf levels were similarly elevated in MDCK^{ARF6-Q} cysts (shown further below).

We questioned whether ERK activation in MDCK^{ARF6-Q} cysts was coupled to the phosphorylation and stabilization of Bcl-2. To this end, cysts were lysed at various stages of development and anti-phosphoserine immunoprecipitates were probed with anti-Bcl-2 (Figure 3A). Increased anti-phosphoserine labeling of Bcl-2 precipitates was observed during later stages of cystogenesis in MDCK^{ARF6-Q} cysts and this coincided temporally with ERK activation. Treatment with PD98059 to inhibit MEK, the kinase immediately upstream of ERK, blocked Bcl-2 phosphorylation (Figure 3B) and fully reversed the reemergence of Bcl-2 expression in MDCK^{ARF6-Q} cysts. Thus, ERK-regulated phosphorylation of Bcl-2, or an associated protein, is responsible for its stabilization. ERK-mediated suppression of Bim, the proapoptotic BCL family protein, has also been shown to promote luminal filling in MCF-10A cells (Reginato *et al.*, 2005). Consistently, Bim expression was blocked during late stages of MDCK^{ARF6-Q} cyst morphogenesis, and this down-regulation also temporally correlated with ERK upregulation (Figure 3A). Finally, $\geq 75\%$ of MDCK^{ARF6-Q} cysts displayed cleared lumens when treated with PD98059 (Figure 3C and Supplemental Figure 4).

Because Bcl-2 phosphorylation by mitogen-activated protein kinases has been thought to protect against ubiquitin-proteasome-mediated degradation (Breitschopf *et al.*, 2000), we examined whether ARF6-GTP cysts contain a smaller pool of ubiquitin tagged Bcl-2 relative to parental cysts. As expected, little to no ubiquitinated Bcl-2 was detected in MDCK^{ARF6-Q} cysts relative to parental cysts at later stages of cyst development (Supplemental Figure 5). Together, these findings demonstrate that ARF6-regulated ERK-dependent phosphorylation of Bcl-2 stabilizes the protein, which may in turn lead to cell survival in cyst lumens.

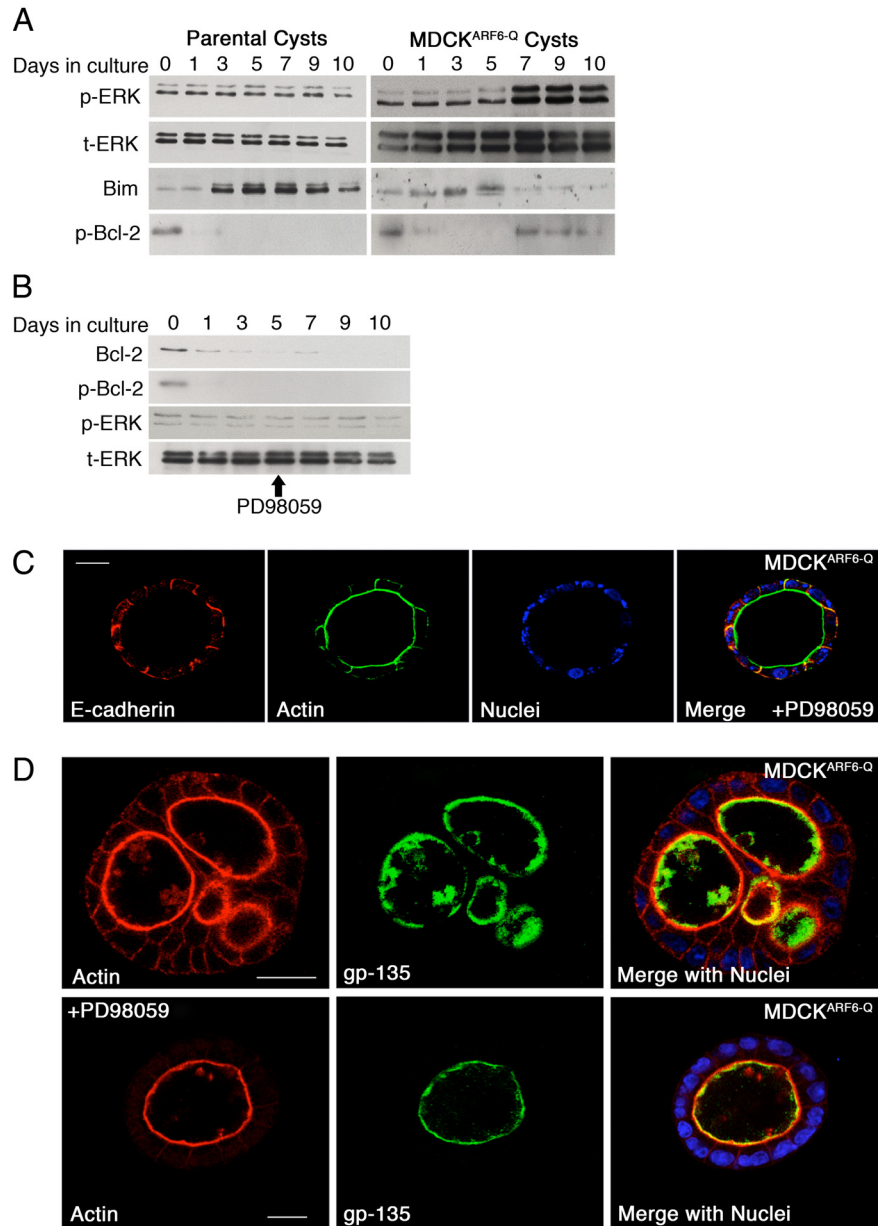


Figure 3. ARF6-induced ERK activation stabilizes Bcl-2 but has no effect on individual cell polarity during cyst development. (A) Parental MDCK and MDCK^{ARF6-Q} cells were cultured in Matrigel to develop cysts and induced for mutant ARF6 expression 2 days after seeding. At the indicated number of days after seeding, developing cysts were harvested and lysed. Equal amounts of cyst lysates were resolved on SDS-PAGE and then blotted for phospho-ERK, total ERK, and Bim. To detect Bcl-2 phosphorylation, the pool of serine-phosphorylated proteins was immunoprecipitated from cyst lysates using anti-phosphoserine antisera, resolved by SDS-PAGE, and blotted with anti-Bcl-2. Down-regulation of Bim and phosphorylation of Bcl-2 coincides with enhanced ERK activation. (B) MDCK^{ARF6-Q} cysts were allowed to develop as described above except that 25 $\mu\text{g/ml}$ PD98059 was added to the culture medium at day 4. Cyst lysates were harvested, resolved by SDS PAGE, and probed for phospho-ERK, total ERK, and Bcl-2. Phosphorylated Bcl-2 was detected as described above. MEK inhibition blocks ERK activation and Bcl-2 up-regulation. (C) MDCK^{ARF6-Q} cysts were allowed to develop in the presence and absence of 25 $\mu\text{g/ml}$ PD98059 as described above. Fully developed cysts at culture day 10 were labeled for actin and E-cadherin as indicated. Cell nuclei are stained in blue. Bar, 10 μm . The majority of MDCK^{ARF6-Q} cysts exhibited clear lumens in the presence of PD98059 (see Supplemental Figure 5). A representative image is shown. (D) MDCK^{ARF6-Q} cysts grown in the presence or absence of PD98059 were labeled for gp135, an apical membrane marker (green) and actin (red). Cell nuclei are stained blue in the merged image. Bar, 10 μm . Gp135 staining is observed exclusively at the apical plasma membrane in both single lumen (PD98059-treated) and multiluminal cysts.

Apical and Basolateral Proteins Are Appropriately Distributed in MDCK^{ARF6-Q} Cysts

In addition to cysts filled with viable cells, the presence of multiple lumens is a striking abnormality of MDCK^{ARF6-Q} cysts. To assess individual cell polarity in MDCK^{ARF6-Q} cysts, we examined the distribution of the apical marker, gp135/podocalyxin. As shown in Figure 3D, in all MDCK^{ARF6-Q} cysts, gp135 labeling was detected exclusively at the cell's apical surface facing the lumen. In addition, proteins at the basolateral surface such as E-cadherin (Figure 1), β_1 -integrin, and β catenin (Supplemental Figure 6) were localized to the correct domain. Thus, apicobasal polarity of individual cells in the cyst is not perturbed, although we cannot exclude the possibility that abnormal ARF6 activation may promote alterations in the trafficking of specific proteins to the appropriate domain.

The lumens observed in MDCK^{ARF6-Q} cysts are largely intercellular and not intracellular as described previously

(Martin-Belmonte *et al.*, 2007). The cellular basis for multiple lumens in MDCK^{ARF6-Q} cysts is less clear but it may result in part by ERK-dependent up-regulation of Bcl-2 leading to cell survival that in turn sterically hinders lumen fusion. These data support the hypothesis that a single lumen may form from a coalescence of multiple lumens. ARF6-GTP-induced alterations in surface protein distribution (such as E-cadherin) could also affect maintenance of lumen integrity.

Treatment of MDCK^{ARF6-Q} cysts with PD98059 resulted in clear lumens with gp135 distribution that completely overlaps with actin (Figure 3D). Thus, as described above, MEK inhibition reverts MDCK^{ARF6-Q} cysts to normalcy, indicating that all changes including the multiple lumen phenotype occur downstream of ERK signaling.

ARF6-induced ERK Activation Requires Phospholipase D

PLD activity is elevated in a large variety of cancers (Foster and Xu, 2003). In response to a variety of mitogenic stimuli,

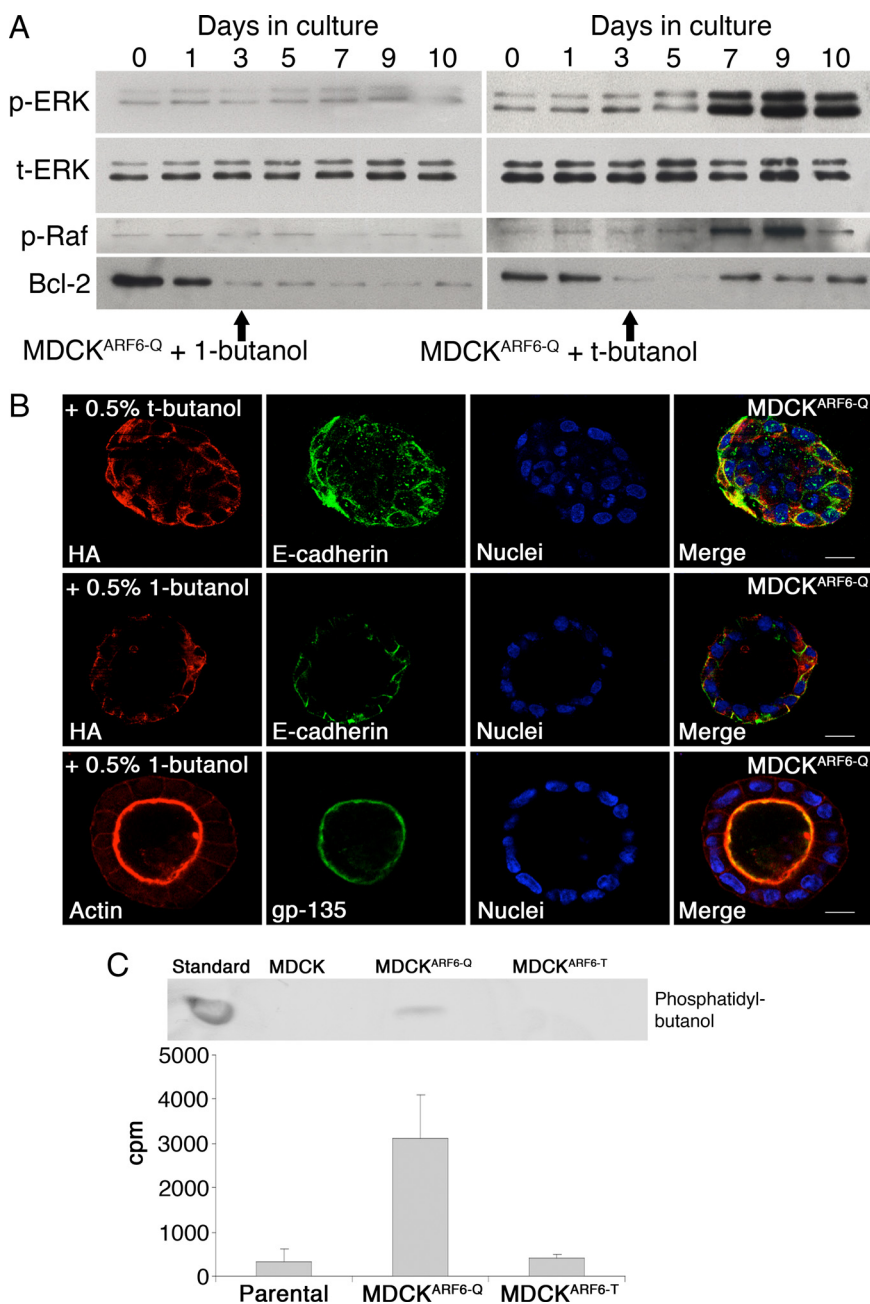


Figure 4. ARF6-regulated ERK activation requires PLD. (A) Parental MDCK and MDCK^{ARF6-Q} cells were cultured in Matrigel to develop cysts. Two days post seeding, cells were induced for mutant ARF6 expression. 1-butanol or *t*-butanol was added to the culture medium at day 3. At the indicated number of days after seeding, developing cysts were harvested and lysed. Equal amounts of cyst lysates were resolved on SDS-PAGE and probed for phospho-ERK, total ERK, phospho-Raf, and Bcl-2. The data are representative of three independent experiments. Primary but not tertiary alcohols block ARF6-GTP-induced ERK activation, which coincides with down-regulation of Raf and Bcl-2 phosphorylation. (B) MDCK^{ARF6-Q} cysts were allowed to develop in the presence or absence of 0.5% 1-butanol or *t*-butanol as indicated. Fully developed cysts were labeled for the HA epitope (red) and E-cadherin (green) or for gp135 (green) and actin (red), as indicated. Cell nuclei are stained blue. Bar, 10 μ m. MDCK^{ARF6-Q} cysts exhibit clear lumens in the presence of primary alcohols. (C) Parental MDCK, MDCK^{ARF6-T} and MDCK^{ARF6-Q} cysts were labeled with [³H]oleic acid and membrane phospholipids were isolated as described. Lipids were separated by TLC and phosphatidylbutanol was identified by comigration with an unlabeled standard. In addition, radiolabeled phosphatidylbutanol on the chromatogram was also quantitated by liquid scintillation counting. The data from three independent experiments is plotted. PLD activity is significantly elevated in MDCK^{ARF6-Q} cysts.

PLD cleaves phosphatidylcholine to generate phosphatidic acid (PA) and choline (Banno, 2002). Both isoforms of PLD, PLD1 and PLD2, have been shown to promote activation of ERK by increasing the membrane-associated pool of phosphorylated Raf (Hong *et al.*, 2001; Andresen *et al.*, 2002).

ARF6 activates PLD and a role for PLD has been described in ARF6-regulated epithelial cell migration, endosome trafficking and regulated secretion (D'Souza-Schorey and Chavrier, 2006). We hypothesized that ARF6-GTP promotes ERK phosphorylation during cyst development by activating PLD activity. To test this hypothesis, MDCK, MDCK^{ARF6-T}, and MDCK^{ARF6-Q} cysts were generated in the presence of 1-butanol or tertiary butanol (*t*-butanol). PLD can use primary alcohols (such as ethanol or 1-butanol), but not secondary or tertiary alcohols, in place of water during the hydrolysis of phosphatidylcholine, producing phosphatidyl-

butanol instead of PA. As shown in Figure 4A, ERK activation was completely blocked in MDCK^{ARF6-Q} cysts in the presence of 1-butanol, but not *t*-butanol. Parallel to its effect on ERK activation, 1-butanol treatment also blocked c-Raf activation (Figure 4A). Consistently, the reemergence of Bcl-2 expression in MDCK^{ARF6-Q} cysts was fully reversed upon PLD inhibition (Figure 4A). Finally, treatment of cysts with 1-butanol resulted in lumen clearance in >75% of cysts; E-cadherin was localized to the basolateral surface and gp135 was distributed appropriately to the apical surface (Figure 4B and Supplemental Figure 4). These results indicate that ARF6-GTP induces increased ERK phosphorylation by activating PLD.

Because the effects of ARF6-GTP on cyst development can be attributed to its activation of PLD, we asked whether PLD activity in MDCK^{ARF6-Q} cysts is higher than in parental MDCK cysts and MDCK^{ARF6-T} cysts. To this end, cysts were

incubated with 1.5 $\mu\text{Ci}/\text{ml}$ [^3H]oleic acid for 24 h, followed by addition of 0.5% 1-butanol to the growth medium for an additional 3 h. Cellular lipids were isolated and analyzed as described in *Materials and Methods*. Phosphatidylbutanol was identified by comigration with an unlabeled standard and quantitated by liquid scintillation counting. We observed a nearly 12-fold increase in tritium incorporation into phosphatidylbutanol in MDCK^{ARF6-Q} cysts (Figure 4C), indicating a significant elevation of PLD activity upon ARF6 activation.

Lysophosphatidyl choline (LPC) is an inverted cone shaped lipid that when exposed on the plasma membrane bends the outer membrane lipids to promote curvature and has been shown to be successful in rescuing a PLD depletion-induced block in cell function, such as regulated exocytosis in PC12 cells (Zeniou-Meyer *et al.*, 2007). As seen in Supplemental Figure 7, with addition of 1 μM LPC to butanol-treated cysts, clear lumens are not observed and the cysts display pheno-

types reminiscent of those induced by ARF6(Q67L) expression. Together, all of the above-mentioned information suggests that PLD functions downstream of ARF6 hyperactivation to facilitate the disruption of epithelial cysts.

ARF6/PLD-regulated Growth Factor Receptor Endocytosis Is Required for Hyperactive ERK Signaling during Cystogenesis

Constitutive signaling resulting from c-Met receptor activation is associated with several epithelial carcinomas (Gentile *et al.*, 2008). Examination of the localization of c-Met in parental MDCK, MDCK^{ARF6-Q}, and MDCK^{ARF6-T} cysts provided key insight into how ARF6 \rightarrow PLD signaling might promote constitutive ERK activation during cyst development. We detected a significant redistribution of the receptor from its normal basolateral membrane localization to intracellular compartments in MDCK^{ARF6-Q} cysts (Figure 5A).

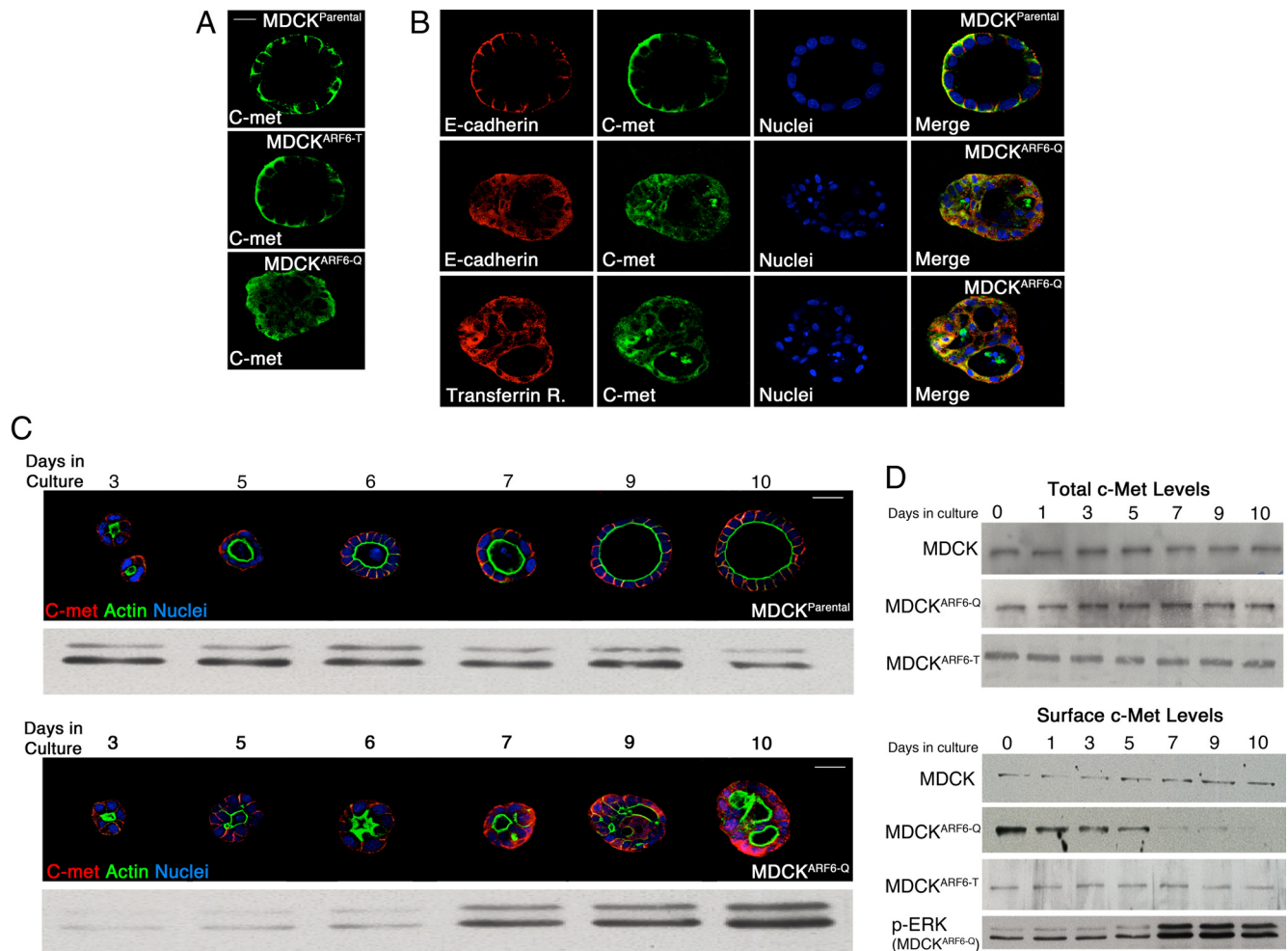
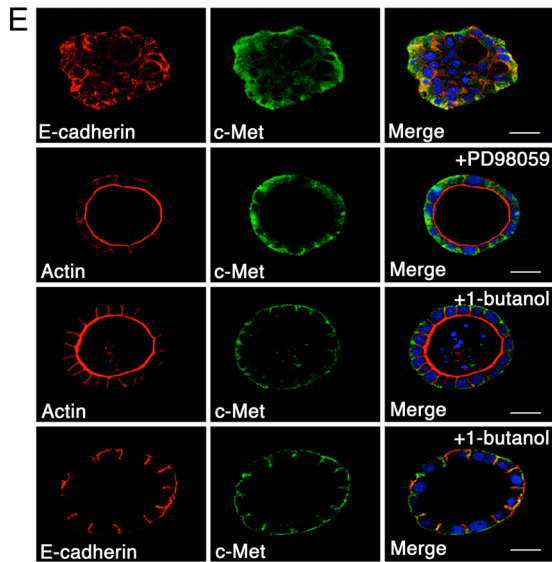


Figure 5. ARF6-GTP promotes receptor internalization into signaling endosomes during cyst development. (A) Mature MDCK, MDCK^{ARF6-T}, and MDCK^{ARF6-Q} cysts were fixed and labeled for c-Met (green). Bar, 10 μm . (B and C) Developing MDCK and MDCK^{ARF6-Q} cysts cultured in Matrigel for the indicated number of days were labeled for c-Met as indicated. Cysts were also stained with FITC-phalloidin to visualize actin distribution (green). Cell nuclei are stained in blue. Bar, 20 μm . Western blots of phospho-ERK levels at corresponding stages of cyst development are also shown. (D) To examine surface levels of c-Met receptor, developing MDCK and MDCK^{ARF6-Q} cysts cultured in Matrigel for the indicated number of days were biotinylated at 0°C, and biotinylated proteins were precipitated as described and probed for c-Met. A phospho-ERK immunoblot (see Figure 3) is shown to illustrate that ERK activation is concomitant with loss of receptor from the cell surface. Total c-Met levels were also determined by Western blotting. (E) Parental MDCK, MDCK^{ARF6-T}, and MDCK^{ARF6-Q} cysts were seeded on Matrigel and mutant ARF6 expression was induced after 48 h. 1-Butanol or PD98059 was added to the culture medium at day 4 where indicated. Mature cysts were labeled for c-Met (green) and E-cadherin or actin (red) as indicated. Cell nuclei are stained blue. Bar, 10 μm . MDCK^{ARF6-Q} cysts develop normally in the presence of PD98059 or 1-butanol. c-Met localizes to the cell surface in the presence of 1-butanol but to intracellular compartments in presence of PD98059.

Figure 5. *Continued.*

These compartments colabeled partially with endocytosed E-cadherin as well as markers for early endosomes such as the transferrin receptor (Figure 5B). Receptor internalization was blocked by expression of an Eps 15 mutant defective in interaction with activator protein 2 (Supplemental Figure 8) or a GTPase-defective dynamin mutant (data not shown). This suggests that c-Met is internalized by clathrin-mediated endocytosis into early endosomes. The redistribution of c-Met was not observed in MDCK^{ARF6-T} cysts consistent with previous findings that dominant negative ARF6 decreases the rate of receptor-mediated endocytosis in polarized epithelial cells (Palacios *et al.*, 2001). The endosomal localization of c-Met in MDCK^{ARF6-Q} cysts is of particular significance in light of emerging evidence that receptors (for ligands such as epidermal growth factor, HGF, insulin-like growth factor, and nerve growth factor) can remain active in early endosomes and moreover, certain signaling events such as ERK activation, require receptor internalization into “signaling endosomes” (Leof, 2000; von Zastrow and Sorokin, 2007). When the distribution of c-Met was analyzed at progressive stages of cyst development, we found a temporal correlation between the steady state distribution of c-Met in intracellular endosomes and ERK activation (Figure 5C). As also evident in Figure 5C, aberrant cyst phenotypes coincided with intracellular c-Met and ERK activation. Note that mutant ARF6 expression is induced at day 3 and the cytoplasmic distribution of receptors slowly increases and steady state internal distribution is attained by day 7. This is accompanied by slight elevation of ERK activation at day 6 but maximal ERK activation at day 7 that correlates temporally with unregulated cell survival, which in turn could interfere with single lumen formation.

The morphological data were further corroborated by biochemical analyses of surface levels of c-Met distribution (Figure 5D). Although the surface distribution of receptors is largely unchanged in normal cysts due to constitutive endocytosis and recycling of receptors, in MDCK^{ARF6-Q} cysts the steady-state distribution of these receptors at the cell surface decreases as accumulation shifts to the cytoplasm. This is consistent with previous observations that ARF6 activation enhances the rate of endocytosis in polarized MDCK cells (Palacios *et al.*, 2002). Of note, total c-Met levels were un-

changed, suggesting that endosomal localization of c-Met was associated with enhanced ERK phosphorylation and aberrant cysts.

Because MEK and PLD inhibition cleared lumens, we examined the effects of MEK and PLD inhibition on c-Met distribution. Inhibition of PLD activity by treatment of MDCK^{ARF6-Q} cysts with 1-butanol, blocked the internalization of c-Met and as such, receptors remained localized to the basolateral cell surface (Figure 5E). PLD inhibition also blocked the internalization of E-cadherin and restored lumen clearance and the normal phenotype. These data suggest the importance of PLD activity in regulating ARF6-mediated internalization of cell surface molecules and corroborate recent findings that PLD can facilitate receptor-mediated endocytosis (Lee *et al.*, 2006). Conversely, treatment of MDCK^{ARF6-Q} cysts with PD98059 had no effect on intracellular c-Met localization although reversion to normal cyst morphology with clear lumens was observed (Figure 5E). Thus, ARF6-stimulated internalization of receptors into intracellular signaling endosomes is dependent on PLD and the steady-state accumulation of signaling endosomes leads to an amplification of downstream signals, in this case, ERK hyperactivation, to promote alterations in cyst development.

To confirm that the reversal to normal phenotype as described above results from a block in receptor endocytosis, we treated MDCK^{ARF6-Q} cysts with dynasore, a cell-permeable inhibitor of dynamin that has been shown to effectively inhibit dynamin-dependent endocytosis (Macia *et al.*, 2006). With dynasore treatment, >80% of MDCK^{ARF6-Q} cysts seemed normal (Supplemental Figure 9). These cysts were smaller relative to cysts formed without dynasore treatment. Parental MDCK cysts treated with dynasore seemed normal but were similarly decreased in size (data not shown). The mean diameter of MDCK cysts in Matrigel is 74.5 μm but is 40.7 μm in the presence of dynasore. We suggest that smaller cysts result because of the decrease in growth-factor receptor signaling when receptor internalization is blocked.

Receptor Localization and ARF6 Activation in Mammary Epithelial Cysts Expressing Activated Growth Factor Receptors

The findings described here suggest that hyperactivation of ARF6 could contribute to alterations in glandular structures that occur during tumor progression. To test whether hyperactivation of growth factor receptors that cause disruption of cyst architecture is associated with constitutive receptor internalization in a more relevant model for cancer, we examined the distribution of CSF-1R in cysts (acini) formed by human mammary epithelial cells in the presence or absence of chronic stimulation with CSF-1 ligand (Wrobel *et al.*, 2004). The MCF-10A cell line was chosen for these studies because CSF-1R expression has been shown to cause loss of cadherin-based cell–cell adhesion and disruption of morphogenesis. Consistent with earlier reports (Wrobel *et al.*, 2004), we found that daily (chronic) stimulation with CSF-1 results in hyperproliferation and disruption of acinar structures (Figure 6A). We also found that hyperstimulated CSF-1 receptors displayed a striking intracellular distribution compared with unstimulated receptors that localize to the basal membrane in normal acini in the absence of chronic stimulation (Figure 6A). Furthermore, endogenous ARF6-GTP levels are elevated in response to chronic ligand treatment (Figure 6B), suggesting that receptor redistribution is accompanied by enhanced activation of ARF6. CSF-induced CSF-1R endocytosis is dependent on ARF6, because dominant-negative ARF6 completely blocks CSF-1R internalization in MCF-10A monolayers (Supplemental Figure 10). We

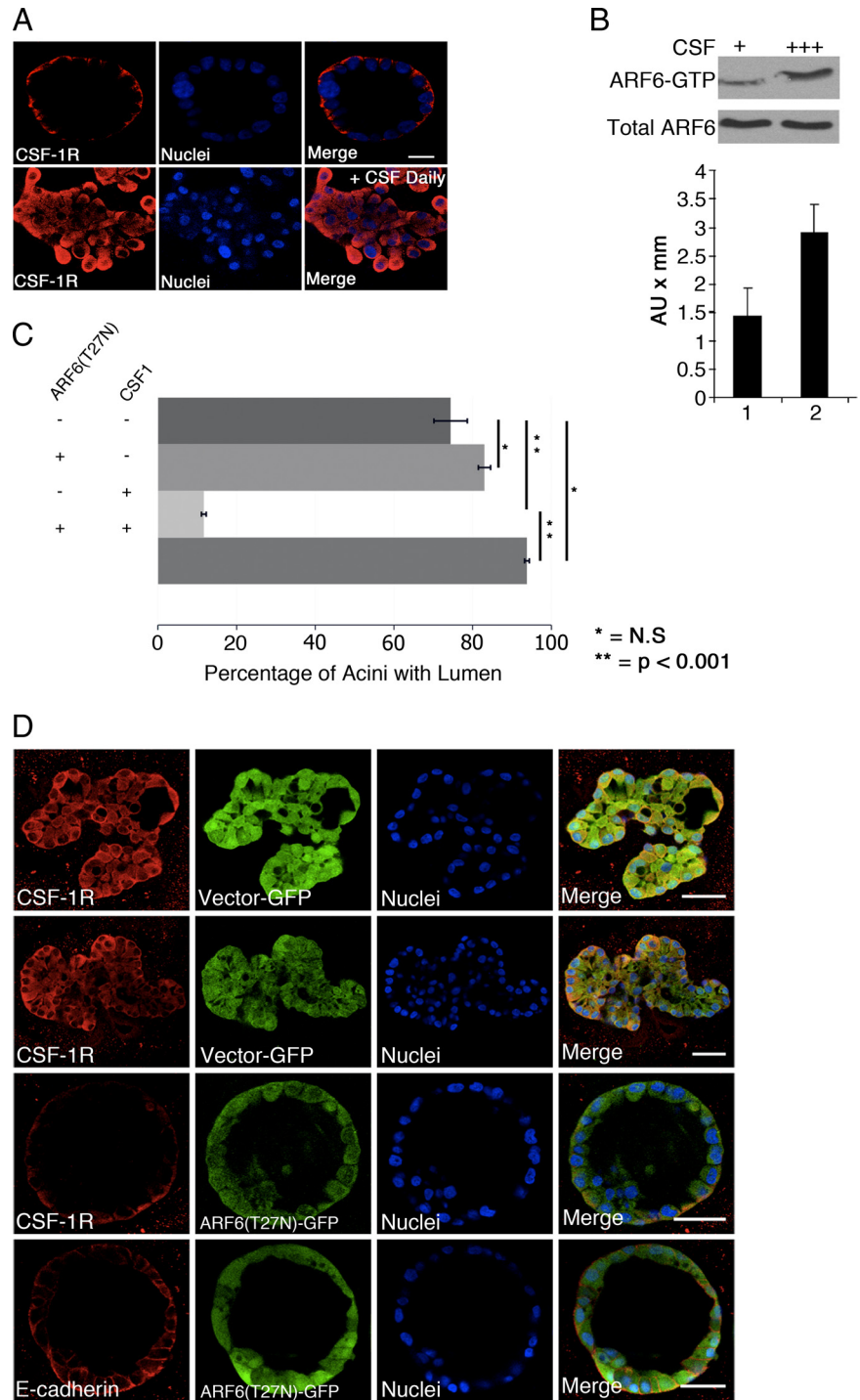


Figure 6. CSF-1 receptors localize to endosomes in disrupted mammary acini and dominant negative ARF6 blocks receptor internalization and acini disruption. (A) MCF-10A cells expressing ectopic CSF-1R were cultured in Matrigel and subjected to chronic stimulation by daily treatment with 10 ng/ml CSF-1. Mature cysts were fixed and labeled for CSF-1R (red) and nuclei (blue). Bar, 20 μ m. Chronic stimulation results in formation of aberrant structures in which receptors localize to intracellular compartments. (B) Acini formed in the presence or absence of chronic stimulation with ligand were lysed, and endogenous ARF6-GTP levels were assessed by the MT2-GST pull-down assay. Total ARF6 levels were determined by Western blotting. ARF6-GTP levels are higher with chronic receptor stimulation whereas total levels are not altered. (C) MCF-10A cells expressing ectopic CSF-1R were cultured in Matrigel and infected with retrovirus encoding ARF6(T27N) and GFP or GFP alone upon seeding. Where indicated, developing cultures were subject to chronic stimulation from day 4 onward. The number of fully developed acini exhibiting single clear lumens along the z-axis was scored and the percentage is shown. At least 50 acini were examined for each condition in a given experiment. *, N.S.; ** $p < 0.001$. (D) Representative images of MCF-10A acini expressing ectopic CSF-1R and infected with retrovirus expressing ARF6(T27N) and GFP or GFP alone is shown. Fully developed acini were labeled for CSF-1R or E-cadherin (red) as indicated. Cell nuclei are labeled blue. Bar, 20 μ m. In the presence of dominant negative ARF6, receptors are largely at the cell surface and the formation of aberrant structures induced by chronic activation with CSF is markedly suppressed.

also we examined whether inhibition of receptor internalization by expression of dominant negative ARF6 would block the effects of chronic CSF stimulation on acini structures. For these studies, MCF-10A cells were infected with retrovirus expressing ARF6(T27N) or GFP alone upon seeding in Matrigel, followed by chronic CSF stimulation at day 4 in culture. Greater than 90% of cysts expressing ARF6(T27N) had single clear lumens (Figure 6C). As observed in the representative images shown in Figure 6D, expression of the ARF6 inhibitory mutant efficiently suppresses chronic CSF-induced hyperproliferation. Notably,

the steady-state distribution of CSF-1R is predominantly at the surface of cysts. Although the signaling pathways by which stimulated CSF-1R leads to proliferative and disorganized glandular structures are not known, we found that treatment with the MEK inhibitor PD98059 partially rescued the abnormal phenotypes induced by chronic CSF-1 stimulation; 85% of PD98059-treated cysts did not exhibit overgrown phenotypes and displayed lumen formation and return of some E-cadherin to the basolateral surfaces (Supplemental Figure 11). Together, these studies show that the accumulation of growth factor receptors in intracellular

compartments, a process that requires ARF6 activation, correlates with disruption of epithelial adhesion and cyst/acini architecture.

DISCUSSION

In this study, we show that constitutive activation of the small GTP-binding protein ARF6 in three-dimensional epithelial cell cultures promotes receptor internalization into signaling endosomes to disrupt normal cyst development. Pronounced perturbations that result from elevated ARF6 activation include filled cysts, multiple lumens and the disruption of cell–cell contacts. The phenotypes induced by ARF6-GTP resemble hallmark histological phenotypes of glandular tumors (Connolly *et al.*, 1989; Debnath and Brugge, 2005). Several reports now indicate that ARF6 activation increases with tumor progression. For example, the screening of various breast tumor cell lines revealed a direct correlation between ARF6 protein expression and invasive capacity (Hashimoto *et al.*, 2004). The ARF6 exchange factor GEP100 is expressed in 70% of primary breast ductal carcinomas and preferentially coexpressed with EGFR in malignant tumors (Morishige *et al.*, 2008). Furthermore, recent work in animal model systems documents a direct correlation between ARF6 activation and tumor progression (Hu *et al.*, 2009; Muralidharan-Chari *et al.*, 2009). Thus, the findings described here could provide a molecular framework to explain how enhanced ARF6-GTP levels in epithelial tumors may contribute to disease pathology.

The phenotypes induced by sustained ARF6 activation can be attributed primarily to its now well-characterized role in facilitating the endocytosis of cell surface molecules (D'Souza-Schorey and Chavrier, 2006). Consistent with previous reports on the effect of ARF6 activation on endocytosis of the cell–cell adhesion molecule, E-cadherin (Palacios *et al.*, 2001, 2002), ARF6-GTP cysts exhibit significant redistribution of E-cadherin to intracellular compartments. In this regard, abnormal expression of E-cadherin in human carcinomas correlates with dedifferentiation, invasion and metastasis although the events responsible for loss of E-cadherin function during cancer progression are still unclear (Birchmeier and Behrens, 1994). Immunohistochemical studies of fixed and frozen tumors show reduced levels of surface E-cadherin staining, although total levels may not be perturbed (Birchmeier and Behrens, 1994; Otto *et al.*, 1994; Cavallaro and Christofori, 2004; Cowin *et al.*, 2005). ARF6-regulated internalization may provide a molecular basis for some of these earlier observations.

ARF6 activation also regulates the internalization of growth factor receptors into signaling endosomes to facilitate pathways that are vital for morphogenesis. However, this study demonstrates that sustained, unregulated ARF6 activation leads to an accumulation of signaling endosomes and thus hyperactive signaling. For example, ERK hyperactivation leads to aberrant phenotypes in MDCK cysts. ARF6 activation is coupled to the constitutive internalization of c-Met in MDCK cysts and CSF-1R in MCF-10A cysts. In both cyst types, intracellular receptor accumulation is accompanied by cyst/acinar structure disruption. Signaling endosomes that form in response to receptor activation, have been described previously (Leof, 2000). Such intracellular signaling platforms can propagate signals during cyst development that are robust, long lived, and highly specific. We propose that receptor localization in signaling endosomes during cyst development is transient, i.e., receptors are continuously internalized and recycled back to the plasma membrane. The steady-state distribution of these

receptors in polarized cysts is largely at the cell surface. However, with increased levels of ARF6-GTP, receptor distribution shifts largely toward intracellular signaling compartments, leading to hyperactive signaling responses.

ARF6-regulated growth factor receptor endocytosis requires PLD. As stated, PLD activity is elevated in a large variety of cancers. PLD can generate lipid intermediates that promote membrane curvature required for vesicle budding, and recent work has also shown that PLD activates the GTPase activity of dynamin through its phox homology domain during receptor endocytosis (Lee *et al.*, 2006). MDCK^{ARF6-Q} cysts exhibit detectably higher levels of PLD relative to parental cysts. Blocking PLD activity in glandular cysts inhibits E-cadherin as well as growth factor receptor internalization, and consequently ERK phosphorylation, thereby leading to lumen clearance. Previous work has shown that ARF6-GTP recruits nm23-H1, a nucleoside diphosphate kinase, to facilitate dynamin-dependent fission at cell–cell contacts (Palacios *et al.*, 2002). It is possible that the effects of ARF6 on PLD and nm23-H1 work in concert to facilitate the generation of signaling endosomes (Figure 7). Treatment of PLD-inhibited MDCK^{ARF6-Q} cysts with LPC partially restores the multiluminal phenotype, reinforcing the importance of PA generation to glandular disruption. We note however that other signaling pathways independent of ARF6 can also generate phosphatidic acid (Foster and Xu, 2003) and may contribute to generation of aberrant phenotypes described here.

MDCK^{ARF6-Q} cysts also exhibit multiple lumens although the molecular basis for this is not fully understood. The multilumen phenotype seems coincident with receptor accumulation in signaling endosomes. Notably, the polarity of individual cells is not perturbed. In fact, as stated earlier, the phenotypes observed raise the speculation that a single lumen may form from a rapid coalescence of multiple lumens, and as such, the lumens seen in MDCK^{ARF6-Q} cysts may represent an intermediate stage of lumen formation. Cell survival in MDCK^{ARF6-Q} cysts induced at least in part by ERK-dependent up-regulation of Bcl-2, may sterically hinder lumen fusion. A direct effect of constitutive ARF6

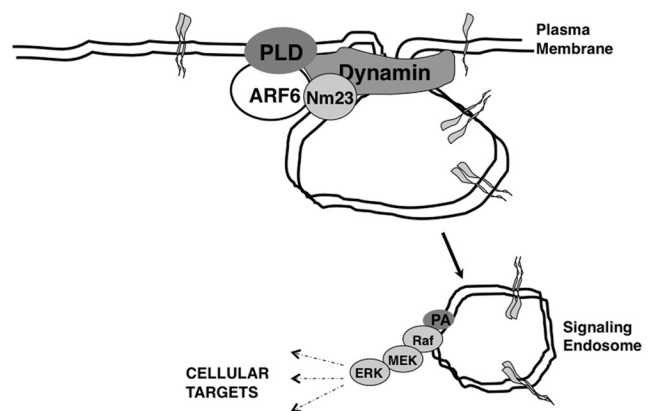


Figure 7. Working model for ARF6-GTP-induced signaling during cyst development. Increased ARF6-GTP levels lead to enhanced PLD activation, and potentially, the recruitment of nm23H1, to facilitate growth factor internalization into signaling endosomes. Signaling endosomes serve as platforms for constitutive receptor signaling. PA enrichment on these vesicular compartments could be important for recruitment of downstream signaling molecules. The type of signaling response elicited is probably dependent on the cell type. In MDCK cysts, elevated ARF6-GTP leads to activation of the ERK signaling pathway.

activation on apical pole organization or some other process resulting in multiple lumens cannot be excluded. For example, the recycling of cargo such as E-cadherin may be required to maintain a single lumen and elevated ARF6-GTP levels would inhibit this process (Palacios *et al.*, 2002). In this regard, the depletion of claudin15, a tight junction associated protein, induced a multiple lumen phenotype in the zebrafish gut due its effect on paracellular transport of fluids (Bagnat *et al.*, 2007). In addition, the depletion of Cdc42 in 3D cultures of intestinal epithelial cysts also generates a multiple lumen phenotype by disrupting spindle orientation of individual cells in cysts (Jaffe *et al.*, 2008). However, it is important to note that a single lumen is restored in MDCK^{ARF6-Q} cysts upon treatment with the MEK inhibitor suggesting that the multilumen phenotype induced by ARF6 activation is dependent on ERK activation.

There is growing evidence for how alterations in endocytic trafficking, particularly of cell surface receptors that initiate signaling pathways involved in proliferation, differentiation, cell survival, and cell motility, result in altered regulation of these processes and therefore become an intricate part of cellular mechanisms that contribute to oncogenesis (Giebel and Wodarz, 2006; Haglund *et al.*, 2007). The studies described here document a role for ARF6 activation and generation of signaling endosomes as mechanisms for constitutive receptor signaling that lead to pathogenic phenotypes of epithelial cysts. They also further understanding of how histological phenotypes demarcating glandular disorganization correlate with specific molecular abnormalities in epithelial cells, and illustrate the value of 3D culture systems in elucidating new mechanisms that result in the disruption of epithelial glandular architecture observed in disease.

ACKNOWLEDGMENTS

We thank Drs. Philippe Chavrier, Keith Mostov, Linda Van Aelst, and Jill Schweitzer for critical reading of the manuscript; Martine Roussel for the CSF-1R and CSF-1 cDNAs; and our laboratories for helpful discussion. J. C. is a GLOBES-National Science Foundation and Lilly Foundation predoctoral fellow, and A. W. is a Siemens Scholar. This work was supported in part by grants from the American Cancer Society and the National Cancer Institute (to C.D.-S.) and a Breast Cancer SPORE and Program Project grant from the National Cancer Institute (to J.S.B.).

REFERENCES

- Andresen, B. T., Rizzo, M. A., Shome, K., and Romero, G. (2002). The role of phosphatidic acid in the regulation of the Ras/MEK/Erk signaling cascade. *FEBS Lett.* 531, 65–68.
- Bagnat, M., Cheung, I. D., Mostov, K. E., and Stainier, D. Y. (2007). Genetic control of single lumen formation in the zebrafish gut. *Nat. Cell Biol.* 9, 954–960.
- Banno, Y. (2002). Regulation and possible role of mammalian phospholipase D in cellular functions. *J. Biochem.* 131, 301–306.
- Birchmeier, W., and Behrens, J. (1994). Cadherin expression in carcinomas: role in the formation of cell junctions and the prevention of invasiveness. *Biochim. Biophys. Acta* 1198, 11–26.
- Bissell, M. J., Rizki, A., and Mian, I. S. (2003). Tissue architecture: the ultimate regulator of breast epithelial function. *Curr. Opin. Cell Biol.* 15, 753–762.
- Breitschopf, K., Zeiher, A. M., and Dimmeler, S. (2000). Ubiquitin-mediated degradation of the proapoptotic active form of bid. A functional consequence on apoptosis induction. *J. Biol. Chem.* 275, 21648–21652.
- Cavallaro, U., and Christofori, G. (2004). Cell adhesion and signalling by cadherins and Ig-CAMs in cancer. *Nat. Rev. Cancer* 4, 118–132.
- Connolly, J. L., Boyages, J., Schnitt, S. J., Recht, A., Silen, W., Sadowsky, N., and Harris, J. R. (1989). In situ carcinoma of the breast. *Annu. Rev. Med.* 40, 173–180.
- Coucouvanis, E., and Martin, G. R. (1995). Signals for death and survival: a two-step mechanism for cavitation in the vertebrate embryo. *Cell* 83, 279–287.
- Cowin, P., Rowlands, T. M., and Hatsell, S. J. (2005). Cadherins and catenins in breast cancer. *Curr. Opin. Cell Biol.* 17, 499–508.
- D'Souza-Schorey, C. (2005). Disassembling adherens junctions: breaking up is hard to do. *Trends Cell Biol.* 15, 19–26.
- D'Souza-Schorey, C., and Chavrier, P. (2006). ARF proteins: roles in membrane traffic and beyond. *Nat. Rev. Mol. Cell Biol.* 7, 347–358.
- Debnath, J., and Brugge, J. S. (2005). Modelling glandular epithelial cancers in three-dimensional cultures. *Nat. Rev. Cancer* 5, 675–688.
- Debnath, J., Mills, K. R., Collins, N. L., Reginato, M. J., Muthuswamy, S. K., and Brugge, J. S. (2002). The role of apoptosis in creating and maintaining luminal space within normal and oncogene-expressing mammary acini. *Cell* 111, 29–40.
- Debnath, J., Muthuswamy, S. K., and Brugge, J. S. (2003). Morphogenesis and oncogenesis of MCF-10A mammary epithelial acini grown in three-dimensional basement membrane cultures. *Methods* 30, 256–268.
- Dimmeler, S., Breitschopf, K., Haendeler, J., and Zeiher, A. M. (1999). De-phosphorylation targets Bcl-2 for ubiquitin-dependent degradation: a link between the apoptosome and the proteasome pathway. *J. Exp. Med.* 189, 1815–1822.
- Foster, D. A., and Xu, L. (2003). Phospholipase D in cell proliferation and cancer. *Mol. Cancer Res.* 1, 789–800.
- Gentile, A., Trusolino, L., and Comoglio, P. M. (2008). The Met tyrosine kinase receptor in development and cancer. *Cancer Metastasis Rev.* 27, 85–94.
- Giebel, B., and Wodarz, A. (2006). Tumor suppressors: control of signaling by endocytosis. *Curr. Biol.* 16, R91–R92.
- Haglund, K., Rusten, T. E., and Stenmark, H. (2007). Aberrant receptor signaling and trafficking as mechanisms in oncogenesis. *Crit. Rev. Oncog.* 13, 39–74.
- Hashimoto, S., Onodera, Y., Hashimoto, A., Tanaka, M., Hamaguchi, M., Yamada, A., and Sabe, H. (2004). Requirement for Arf6 in breast cancer invasive activities. *Proc. Natl. Acad. Sci. USA.* 101, 6647–6652.
- Hong, J. H., Oh, S. O., Lee, M., Kim, Y. R., Kim, D. U., Hur, G. M., Lee, J. H., Lim, K., Hwang, B. D., and Park, S. K. (2001). Enhancement of lysophosphatidic acid-induced ERK phosphorylation by phospholipase D1 via the formation of phosphatidic acid. *Biochem. Biophys. Res. Commun.* 281, 1337–1342.
- Hu, B., Shi, B., Jarzynka, M. J., Yiin, J. J., D'Souza-Schorey, C., and Cheng, S. Y. (2009). ADP-ribosylation factor 6 regulates glioma cell invasion through the IQ-domain GTPase-activating protein 1-Rac1-mediated pathway. *Cancer Res.* 69, 794–801.
- Jaffe, A. B., Kaji, N., Durgan, J., and Hall, A. (2008). Cdc42 controls spindle orientation to position the apical surface during epithelial morphogenesis. *J. Cell Biol.* 183, 625–633.
- Lee, C. S., Kim, I. S., Park, J. B., Lee, M. N., Lee, H. Y., Suh, P. G., and Ryu, S. H. (2006). The phox homology domain of phospholipase D activates dynamin GTPase activity and accelerates EGFR endocytosis. *Nat. Cell Biol.* 8, 477–484.
- Lee, G. Y., Kenny, P. A., Lee, E. H., and Bissell, M. J. (2007). Three-dimensional culture models of normal and malignant breast epithelial cells. *Nat. Methods* 4, 359–365.
- Leof, E. B. (2000). Growth factor receptor signalling: location, location, location. *Trends Cell Biol.* 10, 343–348.
- Lin, H. H., Yang, T. P., Jiang, S. T., Yang, H. Y., and Tang, M. J. (1999). Bcl-2 overexpression prevents apoptosis-induced Madin-Darby canine kidney simple epithelial cyst formation. *Kidney Int.* 55, 168–178.
- Macia, E., Ehrlich, M., Massol, R., Boucrot, E., Brunner, C., and Kirchhausen, T. (2006). Dynasore, a cell-permeable inhibitor of dynamin. *Dev. Cell* 10, 839–850.
- Mailleux, A. A., Overholtzer, M., and Brugge, J. S. (2008). Lumen formation during mammary epithelial morphogenesis: insights from in vitro and in vivo models. *Cell Cycle* 7, 57–62.
- Martin-Belmonte, F., Gassama, A., Datta, A., Yu, W., Rescher, U., Gerke, V., and Mostov, K. (2007). PTEN-mediated apical segregation of phosphoinositides controls epithelial morphogenesis through Cdc42. *Cell* 128, 383–397.
- Morishige, M., *et al.* (2008). GEP100 links epidermal growth factor receptor signalling to Arf6 activation to induce breast cancer invasion. *Nat. Cell Biol.* 10, 85–92.
- Muralidharan-Chari, V., Hoover, H., Clancy, J., Schweitzer, J., Suckow, M. A., Schroeder, V., Castellino, F. J., Schorey, J. S., and D'Souza-Schorey, C. (2009).

- ADP-ribosylation factor 6 regulates tumorigenic and invasive properties in vivo. *Cancer Res.* 69, 2201–2209.
- O'Brien, L. E., Zegers, M. M., and Mostov, K. E. (2002). Opinion: building epithelial architecture: insights from three-dimensional culture models. *Nat. Rev. Mol. Cell Biol.* 3, 531–537.
- Otto, T., Birchmeier, W., Schmidt, U., Hinke, A., Schipper, J., Rubben, H., and Raz, A. (1994). Inverse relation of E-cadherin and autocrine motility factor receptor expression as a prognostic factor in patients with bladder carcinomas. *Cancer Res.* 54, 3120–3123.
- Palacios, F., and D'Souza-Schorey, C. (2003). Modulation of Rac1 and ARF6 activation during epithelial cell scattering. *J. Biol. Chem.* 278, 17395–17400.
- Palacios, F., Price, L., Schweitzer, J., Collard, J. G., and D'Souza-Schorey, C. (2001). An essential role for ARF6-regulated membrane traffic in adherens junction turnover and epithelial cell migration. *EMBO J.* 20, 4973–4986.
- Palacios, F., Schweitzer, J. K., Boshans, R. L., and D'Souza-Schorey, C. (2002). ARF6-GTP recruits Nm23-H1 to facilitate dynamin-mediated endocytosis during adherens junctions disassembly. *Nat. Cell Biol.* 4, 929–936.
- Prigent, M., Dubois, T., Raposo, G., Derrien, V., Tenza, D., Rosse, C., Camonis, J., and Chavrier, P. (2003). ARF6 controls post-endocytic recycling through its downstream exocyst complex effector. *J. Cell Biol.* 163, 1111–1121.
- Pugazhenthhi, S., Nesterova, A., Sable, C., Heidenreich, K. A., Boxer, L. M., Heasley, L. E., and Reusch, J. E. (2000). Akt/protein kinase B up-regulates Bcl-2 expression through cAMP-response element-binding protein. *J. Biol. Chem.* 275, 10761–10766.
- Reginato, M. J., Mills, K. R., Becker, E. B., Lynch, D. K., Bonni, A., Muthuswamy, S. K., and Brugge, J. S. (2005). Bim regulation of lumen formation in cultured mammary epithelial acini is targeted by oncogenes. *Mol. Cell Biol.* 25, 4591–4601.
- Rodrik, V., Gomes, E., Hui, L., Rockwell, P., and Foster, D. A. (2006). Myc stabilization in response to estrogen and phospholipase D in MCF-7 breast cancer cells. *FEBS Lett.* 580, 5647–5652.
- Schweitzer, J. K., and D'Souza-Schorey, C. (2002). Localization and activation of the ARF6 GTPase during cleavage furrow ingression and cytokinesis. *J. Biol. Chem.* 277, 27210–27216.
- Shaw, K. R., Wrobel, C. N., and Brugge, J. S. (2004). Use of three-dimensional basement membrane cultures to model oncogene-induced changes in mammary epithelial morphogenesis. *J. Mammary Gland Biol. Neoplasia* 9, 297–310.
- Tushir, J. S., and D'Souza-Schorey, C. (2007). ARF6-dependent activation of ERK and Rac1 modulates epithelial tubule development. *EMBO J.* 26, 1806–1819.
- van Golen, C. M., Castle, V. P., and Feldman, E. L. (2000). IGF-I receptor activation and BCL-2 overexpression prevent early apoptotic events in human neuroblastoma. *Cell Death Differ.* 7, 654–665.
- von Zastrow, M., and Sorkin, A. (2007). Signaling on the endocytic pathway. *Curr. Opin. Cell Biol.* 19, 436–445.
- Wrobel, C. N., Debnath, J., Lin, E., Beausoleil, S., Roussel, M. F., and Brugge, J. S. (2004). Autocrine CSF-1R activation promotes Src-dependent disruption of mammary epithelial architecture. *J. Cell Biol.* 165, 263–273.
- Zeniou-Meyer, M., Béglé, A., Bader, M. F., and Vitale, N. (2007) Phospholipase D1 production of phosphatidic acid at the plasma membrane promotes exocytosis of large dense-core granules at a late stage. *J. Biol. Chem.* 282, 21746–21757.
- Zheng, Y., Rodrik, V., Toschi, A., Shi, M., Hui, L., Shen, Y., and Foster, D. A. (2006). Phospholipase D couples survival and migration signals in stress response of human cancer cells. *J. Biol. Chem.* 281, 15862–15868.